

Journal Pre-proofs

Crystal structure and microwave dielectric properties in CoO-SnO₂-Nb₂O₅ system

Yun Zhang, Shihua Ding, Tianxiu Song, Yingchun Zhang

PII: S0167-577X(20)30174-9

DOI: <https://doi.org/10.1016/j.matlet.2020.127469>

Reference: MLBLUE 127469

To appear in: *Materials Letters*

Received Date: 5 December 2019

Revised Date: 5 February 2020

Accepted Date: 5 February 2020



Please cite this article as: Y. Zhang, S. Ding, T. Song, Y. Zhang, Crystal structure and microwave dielectric properties in CoO-SnO₂-Nb₂O₅ system, *Materials Letters* (2020), doi: <https://doi.org/10.1016/j.matlet.2020.127469>

This is a PDF file of an article that has undergone enhancements after acceptance, such as the addition of a cover page and metadata, and formatting for readability, but it is not yet the definitive version of record. This version will undergo additional copyediting, typesetting and review before it is published in its final form, but we are providing this version to give early visibility of the article. Please note that, during the production process, errors may be discovered which could affect the content, and all legal disclaimers that apply to the journal pertain.

Crystal structure and microwave dielectric properties in CoO-SnO₂-Nb₂O₅ system

Yun Zhang^{1,*}, Shihua Ding¹, Tianxiu Song¹, Yingchun Zhang²

¹ School of Materials Science and Engineering, Xihua University, Chengdu, China

² School of Materials Science and Engineering, University of Science and Technology Beijing, Beijing, China

Abstract CoSnNb₂O₈ ceramic with medium-permittivity was initially generated. Compositionally induced phase formation was identified by X-ray diffraction. Tetragonal rutile-type CoSnNb₂O₈ was obtained from the reaction of SnO₂ with intermediate phase CoNb₂O₆. Both the dielectric constant ϵ_r and quality factor $Q \times f$ initially increased with the sintering temperature, reaching the maxima at around 1225 °C, and declined thereafter. They were discussed based on the ionic polarizabilities and packing fraction, respectively. The temperature coefficient of resonant frequency τ_f primarily depended on the Nb-site bond valence, as well as oxygen octahedra distortion. When sintered at 1225 °C, the CoSnNb₂O₈ ceramic exhibited optimum properties with $\epsilon_r=31.8$, $Q \times f=43,000$ GHz, and $\tau_f=35.01$ ppm/°C.

Key words: Microwave dielectric property; CoSnNb₂O₈; Sintering; Crystal structure

1. Introduction

Microwave dielectric ceramics have found wide applications as components for mobile system and satellite communication operating at high frequencies. A good dielectric must have appropriate dielectric constant (ϵ_r), high quality factor ($Q \times f$) to improve selectivity, and near-zero temperature coefficient of resonant frequency (τ_f) to minimize frequency drift. [1, 2] Nowadays, the development of low and high

* Corresponding author.
E-mail address: yunzhang_17@163.com

permittivity ceramics is much more advanced than the middle one ($30 < \epsilon_r < 50$). [3]

$M^{2+}M^{4+}Nb_2O_8$ ($M^{2+}=Mg, Co, Ni, Zn$ and $M^{4+}=Ti, Zr$) ceramics are attractive subjects for materials research and engineering applications. [4, 5] Amongst this family, $CoTiNb_2O_8$ was reported to have a high $\epsilon_r \sim 63.5$ and $Q \times f \sim 25,300$ GHz. [4] Its large τ_f was tuned by the addition of $Zn_{1.01}Nb_2O_6$, and additionally, the $Q \times f$ was enhanced to 94,700 GHz. [5] By Ta substitution for Nb, Zhang [6] generated novel trirutile-type $CoTiTa_2O_8$ ceramic. He found that Ta-O bonds with the greatest bond ionicity and lattice energy made the majority contributions to dielectric properties.

Considering the similar ionic radii, extensive importance has also been attached to the replacement of Ti with equivalent-charge Sn. [7] On this basis, the $Q \times f$ increased from 42,500 GHz to 69,500 GHz for $ZnTiNb_2O_8$. [8] More importantly, a 2019 study showed promise of achieving temperature-stable ceramic with single $NiSnTa_2O_8$ phase. [9] The scientific reports indicated that, the replacement not only boosted the microwave properties but also provided feasible access to new dielectrics. In this respect, the microwave dielectric properties of $CoSnNb_2O_8$ ceramic were of special interest. Thus, it was prepared and the property-structure relations were discussed.

2. Experimental procedures

Initial materials CoO (99%), SnO_2 (99%) and Nb_2O_5 (99.99%) were purchased from Aladdin (Shanghai, China). According to the chemical formula, the oxides were milled with zirconium balls in ethanol. The subsequently steps were calcination and re-milling for target products. After being sieved through 200 mesh, the powders were

mixed with 5 wt% polyvinyl alcohol solution. Thereafter, they were pressed into circular disks (10 mm in diameter and 5-6 mm in thickness) with a uniaxial pressure of 100 MPa. During sintering, the temperature was raised to 1175-1275 °C for 4 h.

The sintered densities were identified by Archimedes method. Crystal structure was undertaken via X-ray diffraction (CuK α , D2-PHASER, Bruker). Structural parameters were obtained from Rietveld refinement using GSAS [10]. Scanning electron microscopy (FEI, Quanta 250) recorded the morphology. The ϵ_r was measured using Hakki-Coleman method [11]. The unloaded quality factors were measured with a HP8720ES analyzer. τ_f was obtained in the temperature range from 25 to 85 °C.

3. Results and discussions

Fig. 1 shows XRD spectrums of samples. Calcination at 1000 °C failed to generate single CoSnNb₂O₈ phase, since CoNb₂O₆ (JCPDS NO. 32-0304) were emerged from Fig. 1(a). Increasing temperature accelerated chemical reactions and the amount of residual impurity decreased steadily. The profile displayed a single tetragonal rutile phase at 1100 °C, in agreement with JCPDS file card No. 52-1875. Eqs. (1)-(2) clearly expressed the whole formation process. After sintering process, all diffraction peaks had similar appearances and confirmed the rutile structure [see Fig. 1(b)].



The structural parameters were determined by means of Rietveld method. Representative refinement plot and schematic crystal structure are plotted in Figs. 2(a)

and (b). This structure had only one crystallographic site for metal atoms, which were coordinated with six oxygen atoms. The octahedra were interconnected by edge-sharing, forming infinite linear chains in the *c*-direction. [12] From Fig. 2(d), it was found that there was a reduction in the unit cell volume, between 1175 and 1275 °C.

Fig. 3(a) shows relative densities and SEM of the niobite. When the temperature was 1175 °C, $\text{CoSnNb}_2\text{O}_8$ reached only ~93.68% of the theoretical density. The oval-shaped grains were not well faceted, accompanied by considerable intergranular pores. Higher temperature was likely to promote diffusion kinetics and thereby improved densification. A maximum relative density of 96.89% was achieved at 1225 °C. There was no evidence of pore entrapment. The grain size enlarged rapidly to 13 μm at an even higher temperature of 1275 °C, suggesting exaggerated grain growth.

The microwave dielectric performance of $\text{CoSnNb}_2\text{O}_8$ ceramics is demonstrated in Figs. 3(b)-(d). The measured ϵ_{meas} ranged from 26.7 to 31.8, depending on temperature. The Clausius-Mossotti [13, 14] formula was able to give an theoretical estimate for dielectric constant. In $\text{CoSnNb}_2\text{O}_6$, the ϵ_{cal} was substantially smaller than their measured counterparts. The reason for this discrepancy was the “rattling” or “compressed” cations, as they deprived large or small cation polarizabilities, respectively. [14] The opposite trends (>1225 °C) between ϵ_{cal} and ϵ_{meas} were due to the significant density reduction. Quite similarly, the variations of $Q \times f$ were consistent well with that of relative density. Porosity was a major component of extrinsic dielectric loss. Compounds with enhanced density usually exhibited low loss and vice versa. Besides,

the packing fraction was quantified in current work. With temperature shifting from 1175 to 1225 °C, the $Q \times f$ suggested a similar increasing trend, in compare to packing fraction (Fig. 5). Larger packing fraction was favorable to optimize $Q \times f$. [15] Nevertheless, the consistency was destroyed above 1225 °C. This occurred because 5% porosity was bad enough for $Q \times f$. To be noted that the $Q \times f$ and sintering behavior in this work were superior compared to $\text{CoTiNb}_2\text{O}_8$ [4]. The octahedra distortion and Nb-site bond valence were calculated based on the formulas of Refs [7, 16]. In this case, the Nb-site bond valence depicted an upward trend, which meant higher recovering force for the tilting of NbO_6 octahedra. As a result, the τ_f decreased to 31.44 ppm/°C. The relation of bond valence and τ_f was in line with that previously reported by Kim [15].

Table 1 lists a comparison of the microwave ceramics with $\varepsilon_r \sim 32$. [17-23] Some materials, such as ZnTa_2O_6 [19], $\text{Ba}(\text{Co}_{1/3}\text{Nb}_{2/3})\text{O}_3$ [22] were difficult to densify without any aids. The $Q \times f$ of $\text{CoSnNb}_2\text{O}_8$ might not be the largest in table 1. This ceramic has a lower sintering temperature, making it a promising candidate for dielectric components.

4. Conclusions

The microwave dielectric ceramic $\text{CoSnNb}_2\text{O}_8$ was initially synthesized. Structure-property relations were discussed systemically. The sample with 96.89% theoretical density displayed a tetragonal rutile structure. Depending on the temperature, the ε_r ranged from 26.7 to 31.8. The $Q \times f$ was attributable to the relative density and packing fraction. With the increase of Nb-site bond valence and oxygen octahedron distortion, τ_f moved to the negative direction. In particular, $\text{CoSnNb}_2\text{O}_8$ compound sintered at 1225

$^{\circ}\text{C}$ revealed properties: $\varepsilon_r=31.8$, $Q\times f=43,000$ GHz, and $\tau_f=35.01$ ppm/ $^{\circ}\text{C}$.

Acknowledgements

This work was supported by the National Natural Science Foundation of China (51902268); the Sichuan Science and Technology Program (2019YFG0234).

References

- [1] K. Cheng, C. C. Li, H. C. Xiang, *et al.* Mater. Lett. 228 (2018) 96-99.
- [2] B. Liu, Y. W. Cong, K. Hu, K. X. Song, Mater. Lett. 238 (2019) 245-248.
- [3] T. T. Tao, L. X. W, Q. T. Zhang, J. Alloy. Compd. 486 (2009) 606-609.
- [4] Y. Zhang, Y. C. Zhang, M. Q. Xiang, J. Eur. Ceram. Soc. 36 (2016) 1945-1951.
- [5] Y. Zhang, S. H. Ding, L. You, *et al.*, J. Electron. Mater. 48 (2019) 867-872.
- [6] H. Y. Yang, S. R. Zhang, Y. W. Chen, *et al.*, Inorg. Chem. 58 (2019) 968-976.
- [7] R. D. Shannon, Acta. Cryst. A 32 (1976) 751-767.
- [8] C. F. Xing, J. X. Bi, H. J. Wang, *et al.*, Mater. Lett. 183 (2016) 341-345.
- [9] E. Z. Li, Q. Y. Wen, H. C. Yang, *et al.*, Ceram. Int. (2019) <https://doi.org/10.1016/j.ceramint.2019.11.069>.
- [10] B. H. Toby, J. Appl. Crystallogr. 34 (2001) 210-213.
- [11] B. W. Hakki, P. D. Coleman, Ieee. T. Microw. Theory. 8 (1960) 402-410
- [12] A. Baumgarte, R. Blachnik, J. Alloy. Compd. 215 (1994) 117-120.
- [13] R. D. Shannon, J. Appl. Phys. 73 (1993) 348-366.
- [14] R. D. Shannon, J. E. Dickinson, Phys. Chem. Mineral. 19 (1992) 148-156.
- [15] E. S. Kim, B. S. Chun, R. Freer, *et al.*, J. Eur. Ceram. Soc. 30 (2010) 1731-1736.

- [16] N. E. Brese, M. O'keeffe, *Acta. Cryst. B* 47 (1991) 192-197.
- [17] D. W. Kim, H. B. Hong, K. S. Hong, *et al.*, *Jpn. J. Appl. Phys.* 41 (2002) 6045-6048.
- [18] C. L. Huang, J. F. Tseng, *Mater. Lett.* 58 (2004) 3732-3736.
- [19] A. Kan, H. Ogawa, H. Ohsato, *J. Alloy. Compd.* 337 (2002) 303-308.
- [20] H. T. Kim, M. T. Lanagan, *J. Am. Ceram. Soc.* 86 (2003) 1874-1878.
- [21] Y. R. Wang, S. F. Wang, C. K. Wen, *Mater. Sci. Eng. A* 426 (2006) 143-146.
- [22] F. Azough, C. Leach, R. Freer, *J. Eur. Ceram. Soc.* 26 (2006) 2877-2884.
- [23] D. W. Kim, J. H. Kim, J. R. Kim, *et al.* *Jpn. J. Appl. Phys.* 40 (2001) 5994-5998.

Figure captions

Fig. 1 XRD patterns of (a) CoO-SnO₂-Nb₂O₅ powders calcined at 1000-1100 °C for 4 h and (b) CoSnNb₂O₈ ceramics sintered at 1175-1275 °C for 4 h

Fig. 2 (a) Representative refinement plot; (b) schematic crystal structure; (c) lattice parameters; and (d) V_{unit} for CoSnNb₂O₈ ceramics

Fig. 3 (a) Sintering behavior and corresponding SEM images; (b) ϵ_r ; (c) $Q \times f$; and (d) τ_f vs. sintering temperature of CoSnNb₂O₈ ceramics

Table 1 Comparison of microwave dielectric properties of some ceramics with $\epsilon_r \sim 32$

Composition	$T_s(^{\circ}\text{C})$	ϵ_r	$Q \times f$ (GHz)	τ_f (ppm/ $^{\circ}\text{C}$)	Ref.
BaNb ₂ O ₆	1300	30.0	43,000	-45	[17]
La(Co _{1/2} Ti _{1/2})O ₃	1440	30.0	67,000	-64	[18]
ZnTa ₂ O ₆	1400	30.3	87,580	9.5	[19]
(Zn _{0.5} Co _{0.5})TiO ₃	1150	31.0	60,000	75	[20]
(Zr _{0.8} Sn _{0.2})TiO ₄	1050	31.4	32,000	-1.4	[21]
CoSnNb₂O₈	1225	31.8	43,000	35.01	This work
Ba(Co _{1/3} Nb _{2/3})O ₃	1400	32.0	78,000	-12	[22]
ZnTiNb ₂ O ₈	1250	34.0	42,500	-52	[23]

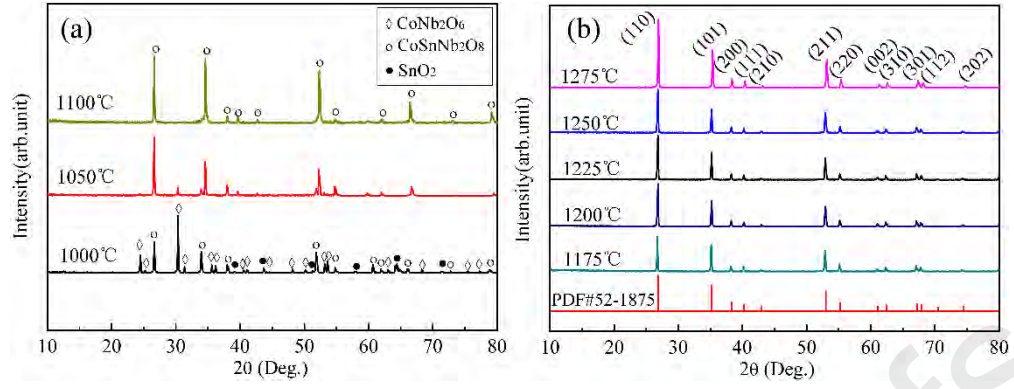


Fig.1

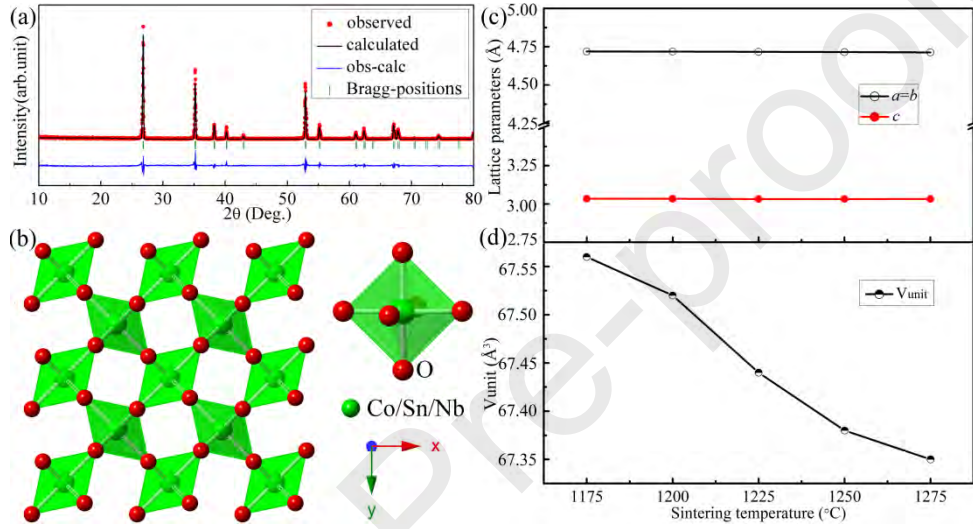


Fig.2

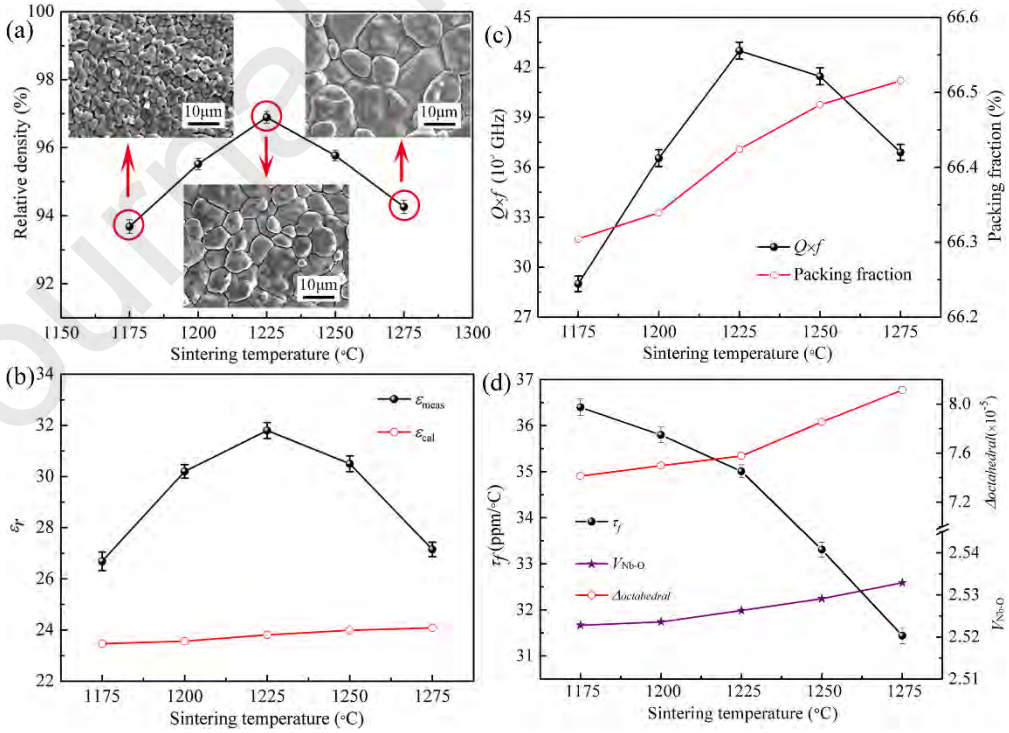


Fig.3

Highlights

CoSnNb₂O₈ ceramic was initially prepared via solid state method.

Structure-property relations were discussed based on Rietveld refinement.

$\epsilon_r=31.8$, $Q \times f=43,000\text{GHz}$, and $\tau_f=35.01\text{ppm}/^\circ\text{C}$ were obtained.

Author contributions

Yun Zhang: Conceptualization, Writing-Reviewing and Editing

Shihua Ding: Investigation, Supervision

Tianxiu Song: Data Curation, Software

Yingchun Zhang: Methodology, Validation

Table 1 Comparison of microwave dielectric properties of some ceramics with $\epsilon_r \sim 32$

Composition	$T_s(^{\circ}\text{C})$	ϵ_r	$Q \times f \text{ (GHz)}$	$\tau_f \text{ (ppm}/^{\circ}\text{C})$	Ref.
BaNb ₂ O ₆	1300	30.0	43,000	-45	[17]
La(Co _{1/2} Ti _{1/2})O ₃	1440	30.0	67,000	-64	[18]
ZnTa ₂ O ₆	1400	30.3	87,580	9.5	[19]
(Zn _{0.5} Co _{0.5})TiO ₃	1150	31.0	60,000	75	[20]
(Zr _{0.8} Sn _{0.2})TiO ₄	1050	31.4	32,000	-1.4	[21]
CoSnNb₂O₈	1225	31.8	43,000	35.01	This work
Ba(Co _{1/3} Nb _{2/3})O ₃	1400	32.0	78,000	-12	[22]
ZnTiNb ₂ O ₈	1250	34.0	42,500	-52	[23]

Declaration of interests

☒ The authors declare that they have no known competing financial interests or personal relationships that could have appeared to influence the work reported in this paper.

☐ The authors declare the following financial interests/personal relationships which may be considered as potential competing interests:

--